

# Molecular nanosprings in spider capture-silk threads

NATHAN BECKER<sup>1</sup>, EMIN OROUDJEV<sup>1</sup>, STEPHANIE MUTZ<sup>1</sup>, JASON P. CLEVELAND<sup>2</sup>,  
PAUL K. HANSMA<sup>1</sup>, CHERYL Y. HAYASHI<sup>3</sup>, DMITRII E. MAKAROV<sup>4</sup> AND HELEN G. HANSMA\*<sup>1</sup>

<sup>1</sup>Department of Physics, University of California, Santa Barbara, California 93106, USA

<sup>2</sup>Asylum Research, 341 Bolay Drive, Santa Barbara, California 93117, USA

<sup>3</sup>Department of Biology, University of California, Riverside, California 92521, USA

<sup>4</sup>Department of Chemistry and Biochemistry and Institute for Theoretical Chemistry, University of Texas at Austin, Austin, Texas 78712, USA

\*e-mail: hhansma@physics.ucsb.edu

Published online: 23 March 2003; doi:10.1038/nmat858

Spider capture silk is a natural material that outperforms almost any synthetic material in its combination of strength and elasticity. The structure of this remarkable material is still largely unknown, because spider-silk proteins have not been crystallized. Capture silk is the sticky spiral in the webs of orb-weaving spiders. Here we are investigating specifically the capture spiral threads from *Araneus*, an ecribellate orb-weaving spider. The major protein of these threads is flagelliform protein, a variety of silk fibroin. We present models for molecular and supramolecular structures of flagelliform protein, derived from amino acid sequences, force spectroscopy (molecular pulling) and stretching of bulk capture web. Pulling on molecules in capture-silk fibres from *Araneus* has revealed rupture peaks due to sacrificial bonds, characteristic of other self-healing biomaterials. The overall force changes are exponential for both capture-silk molecules and intact strands of capture silk.

We often take pride in our ability to create materials that are superior to the ones created by nature. Yet some of the materials that nature creates outperform everything designed by the human mind. The spider's capture silk has tensile strength of ~1 GPa, comparable in strength to Kevlar<sup>1</sup> or steel<sup>2</sup>. Unlike those two man-made materials, however, spider capture silk is also extremely elastic and stretches as much as 500–1,000%<sup>3–5</sup>. With its repeating structural motifs, spider silk is also a natural block copolymer<sup>6</sup>.

Stretchy proteins are particularly interesting from a materials point of view, given the value of elasticity in the design of fabrics, coatings, ropes and fibres, and structural materials<sup>7</sup>. Some stretchy proteins, such as elastin, stretch and relax without any net energy dissipation<sup>8</sup>. These proteins are highly resilient. Other stretchy proteins dissipate energy as heat in the process of stretching and relaxing and are thus less resilient. One advantage of this is that there is less rebound when the elastic protein relaxes. This is desirable in spider capture silk, because excessive rebound would propel the insect away from the web, as if it were on a trampoline<sup>9</sup>.

To capture insects, the two-dimensional (2D) webs of *Araneidae* (orb-weaving spiders) need to be stronger than 3D web-networks of spiders such as the black widow. In 3D webs, the energy required to stop an insect is dissipated primarily by breaking some of the many silk strands. In orb webs, the energy is dissipated not by breaking silk strands but by stretching the elastic capture spiral, which must therefore be strong so that it does not break and release the insect<sup>9</sup>.

Furthermore, the capture-silk spiral must contract readily on stretching so that it does not sag and stick to things as it is blown about by breezes. One of the ways in which capture silk from ecribellate orb-weaving spiders maintains its elasticity is by remaining wet, through the action of its hydroscopic gluey coating. Dry capture silk is much less elastic than wet capture silk. Water acts as a plasticizer or mobilizer for the molecules of capture silk, as shown by solution-state <sup>13</sup>C NMR spectra<sup>10</sup>. Capture silk can also contract from its original length in the web. When contracted to 50% of its original length, the capture silk 'spools' into aqueous droplets on the capture web, producing loops ~100 μm long within the droplet<sup>4</sup>.

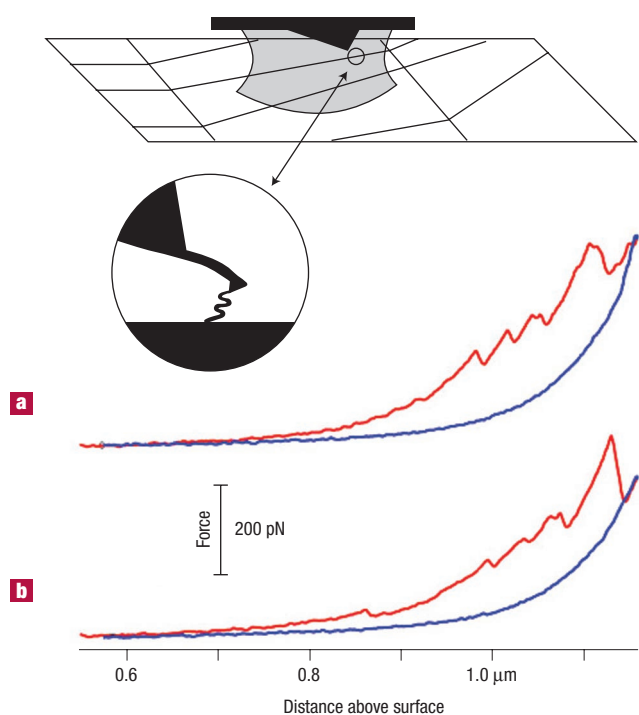


**Figure 1** Force spectroscopy of spider capture-silk molecules. Top: diagram of experimental setup, showing section of a spider web (*Araneus* sp.) deposited onto a glass microscope slide, with a drop of  $\text{CaCl}_2$  solution (10 mM) covering the cantilever and the region of the web that is being pulled. Enlargement (circle) shows detail of cantilever pulling molecules from a region of capture web. **a**, **b**, Two from a series of 36 consecutive pulls on capture silk. Persistence lengths from worm-like chain (WLC) curve fits were typically 0.3–0.5 nm, as observed by other groups when pulling on single protein molecules<sup>18,31</sup>, but this does not exclude the possibility that there was more than one molecule between the tip and surface in these pulls. Another indication of single-molecule pulls is that the force drops to zero at the end of the pull, suggesting that the last molecule stretched between the tip and the surface has just broken away. By this criterion, the pulls here and in Fig. 3 are for a few silk molecules. Upper (red) curve in each pair of curves shows stretching (pulling) of the silk molecules; lower (blue) curve shows retraction (relaxation).

Our new discoveries about the sequence and structure of natural spider capture silk are especially timely with the recent discovery of a way to produce a high-quality synthetic spider dragline silk<sup>11</sup>, something that has had “scientists scheming [to accomplish] for more than 100 years”<sup>12</sup>. We used a relative of the atomic force microscope (AFM) to investigate the molecular and multi-molecular properties of spider capture silk. This instrument, the molecular force probe (MFP), is optimized for the pulling mode and uses AFM cantilevers. Previous AFM-based force spectroscopy<sup>13–16</sup> has revealed the elastic behaviour in molecules of modular proteins such as the muscle protein titin<sup>17,18</sup>, polysaccharides such as cellulose, dextran and amylose<sup>16,19,20</sup>, DNA<sup>21,22</sup>, spider dragline silk<sup>23</sup> and silkworm silk<sup>24</sup>. In addition, spider dragline silk<sup>23,25</sup> and cobweb silk<sup>26</sup> have been imaged by AFM.

We present here the force spectra, or pulling curves, of spider capture-silk molecules (Fig. 1). These force spectra show some of the longest structures seen by force spectroscopy: the longest pulls are over 3  $\mu\text{m}$  long, as compared with typical pulls of several hundred nanometres or less for titin<sup>18</sup> and bone<sup>27</sup>, pulls of  $\sim 200$  nm or less for a dragline silk construct<sup>23</sup>, and pulls of 300–1,200 nm for regenerated fibroin from silkworm silk<sup>24</sup>. The capture-silk force spectra also show

the patterns of elasticity of this spider silk on the smallest force scale yet seen, with pulling forces in the subnanonewton range, as compared with previous forces on capture silk<sup>4</sup> in the range of 1–50  $\mu\text{N}$ . This sensitive force detection was made possible by new instrumentation—MFP and AFM. Pulling results on webs from *Araneus* sp. were combined with capture-silk sequences from *Nephila clavipes*<sup>28</sup> and *Araneus gemmoides* (see Methods) to build molecular and multi-molecular models for capture silk.

In our experiments, a region of unstretched orb web on glass was covered with a drop of fluid (Fig. 1, top). Fluid was important in these pulling experiments, because it eliminated the large meniscus forces occurring in air<sup>29</sup>. It was also appropriate, because capture-silk is coated with a hydroscopic glue that keeps it wet in its natural state<sup>9</sup>. A tip on the end of a cantilever was pressed onto a strand of capture silk lying on the glass slide (see Methods). When the tip picked up one or more molecules from the strand of capture silk, these molecules were then stretched between the tip and the surface of the slide.

After spider-silk molecules were attached to the tip, the tip was raised above the sample surface (nearly 0.6  $\mu\text{m}$  in Fig. 1) to prevent the tip from picking up additional molecules in subsequent cycles of stretching and relaxation. Successive plots of force against extension were then recorded, as in Fig. 1. Thus, the pair of curves in Fig. 1a shows the stretching and relaxation of the same silk molecules. The area between the two curves is a measure of the energy dissipated during one cycle of stretching and relaxing.

Pulls on capture-silk molecules showed a number of saw-teeth (Fig. 1). These saw-teeth were reminiscent of the saw-teeth seen when pulling on the modular proteins titin from muscle<sup>18</sup>, tenascin from the extracellular matrix<sup>17</sup>, spectrin from red blood cells<sup>13</sup>, lustrin in an abalone shell<sup>30</sup>, a synthetic construct of a spider dragline-silk protein<sup>23</sup> and also a non-modular protein, collagen<sup>27</sup>. The saw-teeth in the pulls of these proteins correspond to rupture events, in which sacrificial bonds are broken, exposing previously hidden polypeptide length, and thus reducing the tension on the protein molecules<sup>18,23,30–32</sup>.

The saw-tooth rupture events in pulls on capture-silk persist as the molecule or molecules are cycled through successive pulling and relaxation (Fig. 1). This indicates that sacrificial bonds are being broken and reformed, which suggests that the silk molecules are refolding on relaxation. Thus, spider capture silk seems to be a self-healing biomaterial. Like lustrin in abalone shells, it shows a more irregular pattern of ruptures than titin<sup>18</sup> or synthetic dragline silk<sup>23</sup>. The irregular saw-tooth patterns may be due to a variability in the exact submolecular structure of refolded structures or to the greater complexity of spider capture silk and abalone shell as compared with purified titin and synthetic dragline silk. In each capture-silk pull, the successive rupture peaks usually occurred at increasing forces. The force change between successive rupture peaks showed a broad distribution with a mean of 60 pN (data not shown), equivalent to the rupture force for several hydrogen bonds<sup>33</sup>.

In previously published pulls on titin, spectrin, dragline silk and other proteins, there were nonlinear increases in force preceding the rupture peaks. These nonlinear increases were fitted to the worm-like chain (WLC) model, which is based on the elastic theory of an ideal (non-self-avoiding) polymer stretched in its entropic regime<sup>34–36</sup>.

In contrast, the increases in force preceding the rupture peaks in capture silk were often linear for the intervals of 20–100 nm between two rupture peaks. This linear behaviour was observed in over half of the  $\sim 200$  rupture peaks analysed. Hookian springs have linear force–distance curves, raising the question of whether some rupture peaks in the spider-silk pulls may occur after the stretching of molecular hookian springs.

Hayashi and Lewis predict that molecular springs are the basis for the elasticity of spider capture silk<sup>28,37,38</sup>. Their prediction comes from the spring-like  $\beta$ -spiral sequences of flagelliform protein in capture silk. The flagelliform proteins of *Araneus* (see Methods) and *Nephila*<sup>28</sup> both

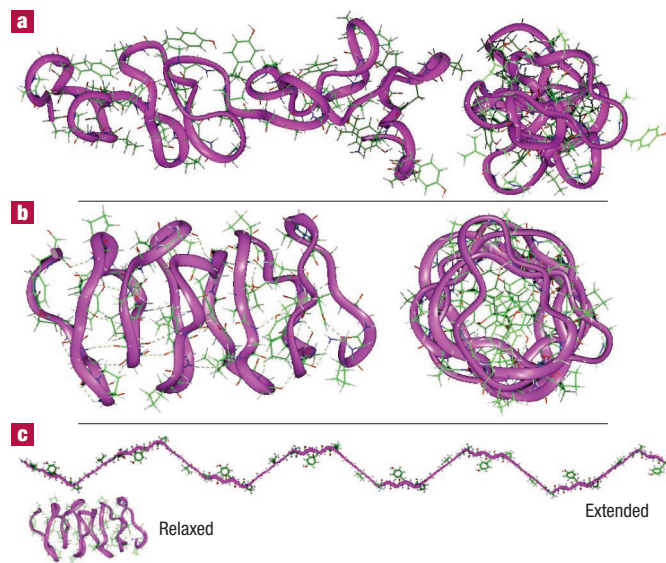


**Figure 2** Molecular models for relaxed and extended flagelliform protein sequences from spider capture silk. **a, b**, Side and end views for possible flagelliform protein conformations of (a) *Araneus gemmoides*, 85 amino acids long (sequence is VPGGAGYGPGGVYGPAGGSLSGPGGAGPYGGVGPGGAGPYGGVGPGGAGPYGGVGP GGAGPYGGVGP GGAGPYGGV), and (b) *Nephila clavipes*<sup>28</sup>, 75 amino acids long, (GPGGX)<sub>15</sub>, where X is Y or V, alternately. **c**, Scale models for extended and relaxed GPGGX sequences, 75 amino acids long. The extended model is at the maximum extension of the protein, without deforming bond angles. The highly repetitive  $\beta$ -spiral sequence forms almost 90% of the ~440-amino-acid-long domains of *Nephila* flagelliform protein. The remaining 10% is a short highly conserved spacer sequence rich in acidic amino acids. There are at least 13 of these  $\beta$ -spiral domains in series in a single molecule of spider capture silk, based on DNA sequences from *Nephila clavipes* and *N. madagascariensis*<sup>28</sup>. The flagelliform protein in spider capture silk is coated with an aqueous glue. The glue contains a high concentration of positively charged organic amines and diamines, and also glycoproteins rich in N-acetylgalactosamine<sup>43,44</sup>.

contain high percentages of glycine and proline, often in the repetitive GPGGX<sub>n</sub> motifs characteristic of  $\beta$ -spirals.

Model structures for flagelliform proteins in Fig. 2 were designed with the assumptions that  $\beta$ -spirals were present and that the unstretched proteins were compact, allowing for considerable elongation, as observed from the extreme elasticity of both bulk capture silk<sup>3–5,39</sup> and its molecules (Fig. 1).  $\beta$ -spiral models of flagelliform-protein sequences from *Araneus gemmoides* (Fig. 2a) reflect the fact that its sequence is less regular than the *Nephila clavipes* sequence, modelled in Fig. 2b. Relaxed and extended conformations (Fig. 2c) show the large change in length that can occur with extension. Single molecules of capture silk are composed of tandem repeats of the entire ensemble, consisting of repetitive  $\beta$ -spiral sequences plus non-repetitive spacer sequences, as shown in the diagram in Fig. 2d.

Even if the elasticity of capture silk is due to  $\beta$ -spirals acting as molecular springs, these springs are not necessarily hookian. They may, instead, function primarily as entropic springs<sup>37</sup>. In work in progress, we are carrying out simulated pulling, using steered molecular dynamics, to investigate the molecular origins of the unique mechanical properties of the  $\beta$ -spiral sequences in flagelliform protein. Unlike a metal spring, a polypeptide ‘spring’ has a backbone that is, in theory, free to rotate around its C–C and C–N single-bonds. The prevalence of prolines in the flagelliform sequence, and the side chains of the amino acids, will hinder the free rotation of the

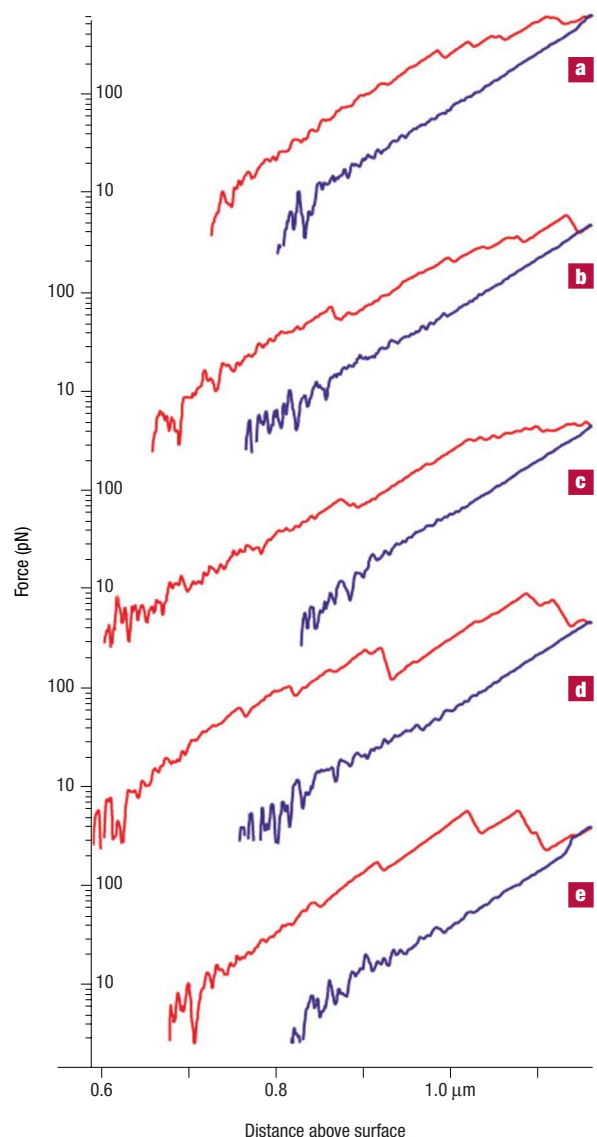


**Figure 3** Force changes for stretching and relaxation of spider capture-silk molecules. Force changes are exponential over a force range from a few pN to ~500–800 pN. The force scales are on alternate sides of the y-axis such that scales for **a, c and e** are on the inside and scales for **b and d** are on the outside of the y-axis. **a and b** show the same data sets as Fig. 1a and b, and **c–e** are the next three data sets in this series. As in Fig. 1, upper and lower curves of each force-distance pair show stretching and relaxation, respectively. Exponential curve fits for relaxation curves had correlation coefficients  $R > 0.990$ . The length constants were calculated for the relaxation curves from the exponential equation,  $F = F_0 \exp(x/x_0)$  where  $F$  is the force at extension  $x$ ;  $F_0$  is the initial force and  $x_0$  is the length constant. The length constant  $x_0$  is longer for pulls further from the surface.

polypeptide backbone; but this does not ensure that there is any hookian component to the backbone elasticity.

The WLC was a bad fit for many of the force increases preceding rupture peaks; it was also a bad fit for the overall force changes during pulling. To a first approximation, the forces increased exponentially with pulling, and decreased exponentially with relaxation, over a range of forces from several piconewtons to as high as 800–900 pN (Fig. 3). The rupture peaks appeared as force maxima, followed by force drops,

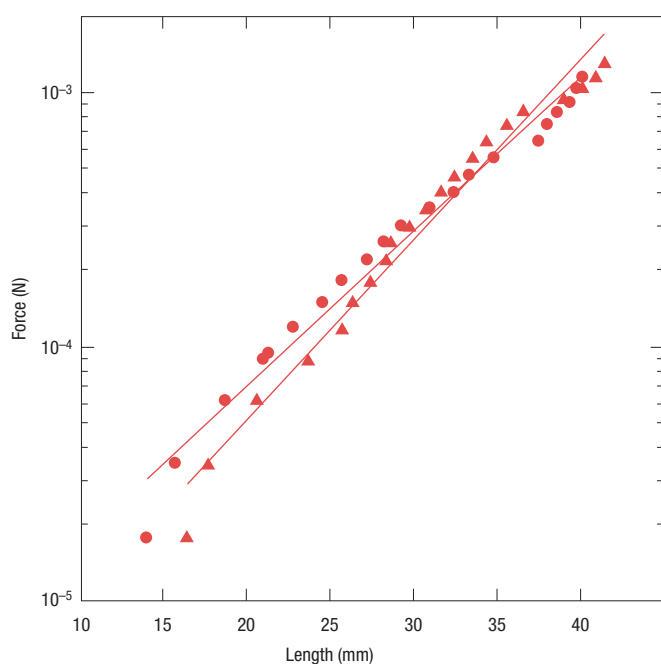


**Figure 4** Force increases are exponential for stretching intact spider capture silk in air. Circles and triangles are data from two regions of capture webs.

along the exponential pull curves. The length constants calculated for the relaxation curves were  $110 \pm 30$  nm ( $n = 31$ ). WLC fits (not shown) were significantly worse than exponential fits for all of the relaxation curves of Fig. 3 and many segments of the pulling curves. WLC fits have been used to characterize pulling and relaxation curves for the proteins titin, tenascin and spectrin<sup>13,17,18</sup>; capture-silk molecules thus show a different behaviour.

On the largest scale—intact capture silk—we also obtained exponential force–distance curves (Fig. 4). The distance constant was  $11 \pm 3$  mm ( $n = 12$ ) for stretching intact spider capture silk in air. This exponential force increase is consistent with Vollrath's early work on stretching intact spider capture silk<sup>4</sup>. Vollrath's capture-silk pull also shows an initial length increase at very low force before the roughly exponential force increase. This length increase may be due to the unwinding of extra capture-silk length from the 'windlass' or 'spool' that Vollrath observes in the glue droplets of capture silk<sup>4</sup>. In contrast, intact spider dragline silk does not show an exponential force increase on stretching<sup>40</sup>.

What picture emerges for capture silk that might explain the exponential force–distance curves seen both when pulling on one or a few molecules and when stretching intact capture silk? These two sets of exponential data are easier to reconcile if we propose that the force-spectroscopy pulls are of more than one molecule, because the intact capture silk is clearly composed of multiple molecules.

One possible model is that we are stretching several of these sticky proteins that successively rupture or detach, sometimes even in multiple steps because of looping. At the high extensions where we analyse the data, the proteins might be unfolded, in which case the slope would be determined by the elasticity of the protein backbones. Standard models for the elasticity of unfolded proteins are based on entropic arguments in combination with enthalpic contributions. Freely jointed chain (FJC), WLC and exponential curves all converge at high forces and high extensions<sup>41</sup>. The exponential fit of the data is therefore necessary but not sufficient to claim a non-entropic nature of the elastic response.

Additional information, such as the temperature dependence, would help to strengthen this claim.

An alternate model is a molecular network composed of interconnected springs. To see how such a network can lead to an exponential force–extension curve, consider the system of identical springs shown in Fig. 5a. Each spring has a spring constant  $k$  and unfolds at force  $f$ ; its length increases by a length  $L$  when it unfolds. As the force  $F$  applied to the system is increased, unfolding events will take place at  $F = f, 2f, 4f, \dots, 2^n f$ , with the resulting extension of the system being  $L, 2L, 3L, \dots, (n + 1)L$ . The overall force constant after the rupture events will be  $k, 2k, 4k, \dots, 2^n k$ . Thus the overall dependence of the force on the extension is exponential. In spider webs, this exponential force increase may occur if one pulls not on a single chain but on a collection of chains joined by crosslinks, as in Fig. 5b. If such a crosslinked network is pulled, its properties may be similar to the model in Fig. 5a. This model assumes the existence of hookian springs, whose presence in capture silk is highly hypothetical, as discussed above. The problem of capture silk's structure is not a simple one, but these two different models can serve as springboards for designing better models and new experiments.

Crosslinks between molecules may come from spacer sequences in the capture silk, as shown in Fig. 2b. The spacer sequences in *Nephila clavipes* are highly conserved and are relatively rich in the acidic amino acids Asp and Glu<sup>28,38</sup>; only one spacer sequence is known for *Araneus gemmoides*, and it also has Asp (D) and Glu (E) (see Methods section on molecular modelling; spacer sequence is in bold type). Salt bridges between these acidic amino acids could provide attachments between adjacent flagelliform molecules. In mussel byssus threads, crosslinks form between histidine residues chelated to divalent inorganic cations<sup>42</sup>. In flagelliform protein, no divalent inorganic cations were detected by either SIMS (secondary ion mass spectrometry) or XPS (X-ray photoelectron spectroscopy); Na<sup>+</sup> and K<sup>+</sup> were the only

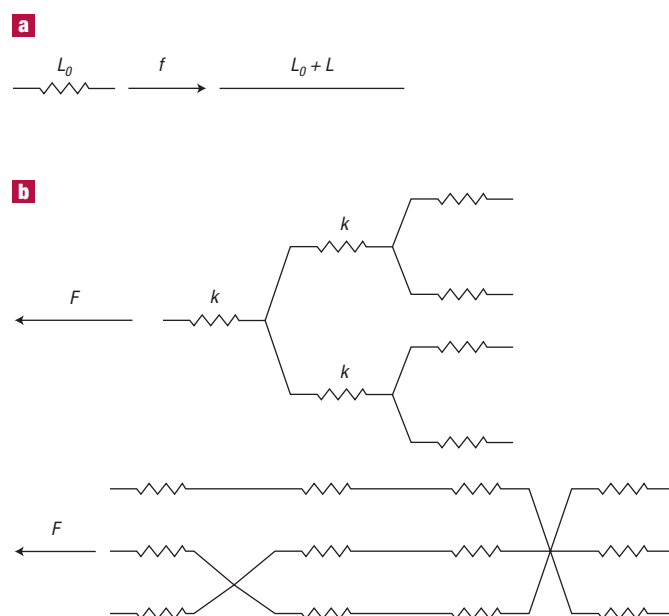


**Figure 5** Schematic diagram for a network of identical springs that gives exponential force–distance curves on stretching. Each spring, of length  $L_0$  and spring constant  $k$ , increases by length  $L$  under a stretching force  $f$ .  $F$  is total force applied to a network,  $N$  is number of springs in network (see text). **a**, Idealized network; **b**, example of a hypothetical network in spider capture silk.



inorganic cations observed (S.M. and E.O., unpublished results). In capture silk, the crosslinks may be components of the capture-silk glue, such as the organic diamines or the amino-sugars of the glue glycoproteins<sup>43,44</sup>.

Spider capture silk is not the only biopolymer that shows exponential force increases with pulling. Single-stranded DNA also stretches exponentially, especially at large extensions or when it is in a fluid of low ionic strength<sup>41</sup>. This is, as Bensimon says, a 'real' polymer, more complex than the ideal (non-self-avoiding) polymers that are modelled nicely by WLC or FJC models<sup>34</sup>. These deviations from WLC and FJC polymer models have been attributed to excluded volume effects caused by polymer self-avoidance<sup>34,41,45</sup>.

In conclusion, spider silk is an extraordinary natural material that has been around for almost 400 million years<sup>46</sup>, since long before the time of dinosaurs. Many silk protein sequences have remained highly conserved for an extremely long time<sup>47</sup>. There must be a strong reason for the sequences to be so highly conserved, and it probably relates to the essential materials properties of spider silks and spider webs. With a relatively new technique—force spectroscopy—and extensive analysis of the pulls and the amino-acid sequence, we have proposed models for both the molecular and the multimolecular structures of capture silk. Capture silk is harder to investigate than the less-elastic dragline silk, because capture silk is found only in orb webs and is thus difficult to isolate from dragline silk. Therefore force spectroscopy is especially valuable, because it can be used to investigate capture silk *in situ* in orb webs.

## METHODS

### PULLING CAPTURE-SILK MOLECULES UNDER FLUID

A section of spider web from *Araneus* sp. was deposited onto a clean glass microscope slide by holding the slide against the web and carefully breaking off silk strands at the edges of the slide. Webs on slides were stored in a dust-free container under ambient conditions until used for pulling. For pulling, the slide was mounted in the MFP (MFP-SA, Asylum Research, Santa Barbara), and a few drops of aqueous CaCl<sub>2</sub> (10 mM) were pipetted onto a V-shaped silicon nitride cantilever (spring constant  $k \approx 30$  pN nm<sup>-1</sup>) and onto a strand of capture web attached to the glass slide. The MFP head with the cantilever was lowered onto the MFP base with the glass slide. The optics of the MFP are readily able to image the capture silk and its glue-droplets, which were spaced at intervals of  $\sim 100$   $\mu$ m. The glue surrounding the capture web was typically washed away by the aqueous fluid covering the web. The cantilever was manually lowered to the capture web, and the MFP was operated such that the cantilever moved away from and then towards the sample surface during the course of each pull. Simply pressing the cantilever's tip onto a capture-silk strand was sufficient for stretching molecules between the tip and the surface, as has been observed previously with other biomaterials<sup>23,32,48</sup>.

### MOLECULAR MODELLING OF FLAGELLIFORM PROTEIN SEQUENCES

Modelling was done with Insight II (Molecular Simulations) essentially as described previously<sup>49</sup>. The sequence from *Nephila clavipes* was modelled as  $\beta$ -strands with Type II turns with modified psi and phi angles for G3–G4 in GPGG repeats. This model forms folds for the *Nephila* sequence with many hydrogen bonds stabilizing the  $\beta$ -spiral, and with all side chains facing towards the inside of the spiral, thus providing additional stabilization for this fold in an aqueous environment. Other folds also gave compact model structures for the *Nephila* sequence, but some had problems such as a low number of hydrogen bonds and side chains exposed to the outside rather than the inside of spirals. The sequence from *Araneus gemmoides* was modelled with Type II' turns. The entire cDNA sequence for *Araneus gemmoides*, whose middle 85 amino acids were modelled in Fig. 2b, is GPGGV[GPGGAGV]<sub>n</sub>GPGGAYGPGGVYGPAGGLS[GPG-GAGPYGPGGV]<sub>n</sub>GPGGAGFGPGGAPGAP[GPG]<sub>n</sub>GPGGVGGPLGPGAGGVGPGGAGPYGPG-GAGPGGVGPGGAGPYGPGGPGGAGPGGEGPVTVDVEVNVGGAPGG; the spacer sequence is in bold type. This is the sequence for one of the tandemly arrayed ensemble repeats from the cDNA library made from the flagelliform gland mRNA: The amino acid composition of this sequence is similar to the composition reported<sup>30</sup> for *Araneus diadematus*, which has 44% G, 21% P, 8% A, 7% V, 3% each of D, G, S, T; and 1% each of R, L.

### PULLING INTACT CAPTURE-SILK IN AIR

A region of web was captured onto an open plastic grid with 1-cm squares. Regions of capture web that spanned a square were fixed with epoxy to the square at each end, to prevent slippage. The plastic grid was suspended above the stage of a dissecting microscope. Force on the web was increased by hooking small wire weights to the web. Length increases were measured from the changes in height of the microscope head when the lowest point of the web was in focus. Data for force against extension were calculated from these measurements.

Received 22 October 2002; accepted 18 February 2003; published 23 March 2003.

## References

- Hinman, M. B., Jones, J. A. & Lewis, R. V. Synthetic spider silk: a modular fiber. *Trends Biotechnol.* **18**, 374–379 (2000).
- Handbook of Chemistry and Physics* (eds Weast, R. C., Selby, S. M. & Hodgman, C. D.) F-15 (Chemical Rubber, Cleveland, Ohio, 1965).

- Opell, B. D. & Bond, J. E. Capture thread extensibility of orb-weaving spiders: Testing punctuated and associative explanations of character evolution. *Biol. J. Linn. Soc.* **70**, 107–120 (2000).
- Vollrath, F. & Edmonds, D. T. Modulation of the mechanical properties of spider silk by coating with water. *Nature* **340**, 305–307 (1989).
- Kohler, T. & Vollrath, F. Thread biomechanics in the two orb-weaving spiders *Araneus diadematus* (Araneae, Araneidae) and *Uloborus walckenaerius* (Araneae, Uloboridae). *J. Exp. Zool.* **271**, 1–17 (1995).
- Jelinski, L. W. et al. Orientation, structure, wet-spinning, and molecular basis for supercontraction of spider dragline silk. *Int. J. Biol. Macromol.* **24**, 197–201 (1999).
- Alper, J. Protein structure: Stretching the limits. *Science* **297**, 329–331 (2002).
- Urry, D. W. et al. Elastin: A representative ideal protein elastomer. *Phil. Trans. R. Soc. Lond. B* **357**, 169–184 (2002).
- Vollrath, F. Spider webs and silks. *Sci. Am.* **266**, 70–76 (1992).
- Bonthrone, K. M., Vollrath, F., Hunter, B. K. & Sanders, J. K. M. The elasticity of spiders' webs is due to water-induced mobility at a molecular level. *Proc. R. Soc. Lond. B* **248**, 141–144 (1992).
- Lazaris, A. et al. Spider silk fibers spun from soluble recombinant silk produced in mammalian cells. *Science* **295**, 472–476 (2002).
- Service, R. F. Mammalian cells spin a spidery new yarn. *Science* **295**, 419–421 (2002).
- Rief, M., Pascual, J., Saraste, M. & Gaub, H. E. Single molecule force spectroscopy of spectrin repeats: low unfolding forces in helix bundles. *J. Mol. Biol.* **286**, 553–61. (1999).
- Engel, A. & Muller, D. J. Observing single biomolecules at work with the atomic force microscope. *Nature Struct. Biol.* **7**, 715–718 (2000).
- Fisher, T. E., Marszalek, P. E. & Fernandez, J. M. Stretching single molecules into novel conformations using the atomic force microscope. *Nature Struct. Biol.* **7**, 719–724 (2000).
- Rief, M., Oesterhelt, F., Heymann, B. & Gaub, H. E. Single molecule force spectroscopy on polysaccharides by atomic force microscopy. *Science* **275**, 1295–1297 (1997).
- Oberhauser, A. F., Marszalek, P. E., Erickson, H. P. & Fernandez, J. M. The molecular elasticity of the extracellular matrix protein tenascin. *Nature* **393**, 181–185 (1998).
- Rief, M., Gautel, M., Oesterhelt, F., Fernandez, J. M. & Gaub, H. E. Reversible unfolding of individual titin immunoglobulin domains by AFM. *Science* **276**, 1109–1112 (1997).
- Grandbois, M., Beyer, M., Rief, M., Clausen-Schaumann, H. & Gaub, H. E. How strong is a covalent bond? *Science* **283**, 1727–1730 (1999).
- Marszalek, P. E., Oberhauser, A. F., Pang, Y. P. & Fernandez, J. M. Polysaccharide elasticity governed by chair–boat transitions of the glucopyranose ring. *Nature* **396**, 661–664 (1998).
- Lee, G. U., Chrissy, L. A. & Coulton, R. J. Direct measurement of the forces between complementary strands of DNA. *Science* **266**, 771–773 (1994).
- Rief, M., Clausen-Schaumann, H. & Gaub, H. E. Sequence-dependent mechanics of single DNA molecules. *Nature Struct. Biol.* **6**, 346–9 (1999).
- Orudjev, E. et al. Segmented nanofibers of spider dragline silk: atomic force microscopy and single-molecule force spectroscopy. *Proc. Natl Acad. Sci. USA* **99**, 6460–6465 (2002).
- Zhang, W. K. et al. Single-molecule force spectroscopy on *Bombyx mori* silk fibroin by atomic force microscopy. *Langmuir* **16**, 4305–4308 (2000).
- Li, S. F. Y., McGhie, A. J. & Tang, S. L. New internal structure of spider dragline silk revealed by atomic force microscopy. *Biophys. J.* **66**, 1209–1212 (1994).
- Gould, S. A. C., Tran, K. T., Spagna, J. C., Moore, A. M. F. & Shulman, J. B. Short and long range order of the morphology of silk from *Latrodectus hesperus* (Black Widow) as characterized by atomic force microscopy. *Int. J. Biol. Macromol.* **24**, 151–157 (1999).
- Thompson, J. B. et al. Bone indentation recovery time correlates with bond reforming time. *Nature* **414**, 773–776 (2001).
- Hayashi, C. Y. & Lewis, R. V. Molecular architecture and evolution of a modular spider silk protein gene. *Science* **287**, 1477–1479 (2000).
- Drake, B. et al. Imaging crystals, polymers, and processes in water with the atomic force microscope. *Science* **243**, 1586–1589 (1989).
- Smith, B. L. et al. Molecular mechanistic origin of the toughness of natural adhesives, fibres and composites. *Nature* **399**, 761–763 (1999).
- Fisher, T. E., Oberhauser, A. F., Carrion-Vazquez, M., Marszalek, P. E. & Fernandez, J. M. The study of protein mechanics with the atomic force microscope. *Trends Biochem. Sci.* **24**, 379–384 (1999).
- Best, R. B., Li, B., Steward, A., Daggett, V. & Clarke, J. Can non-mechanical proteins withstand force? Stretching barnase by atomic force microscopy and molecular dynamics simulation. *Biophys. J.* **81**, 2344–56 (2001).
- Hoh, J. H., Cleveland, J. P., Prater, C. B., Revel, J.-P. & Hansma, P. K. Quantized adhesion detected with the atomic force microscope. *J. Am. Chem. Soc.* **114**, 4917–4918 (1992).
- Dessinges, M.-N. et al. Stretching single stranded DNA, a model polyelectrolyte. *Phys. Rev. Lett.* **89**, 248102 (2002).
- Bustamante, C., Marko, J. F., Siggia, E. D. & Smith, S. Entropic elasticity of lambda-phage DNA. *Science* **265**, 1599–1600 (1994).
- Marko, J. F. & Siggia, E. D. Stretching DNA. *Macromolecules* **28**, 8759–8770 (1995).
- Lewis, R. V. & Hayashi, C. Y. US Patent 5,994,099 in *Official Gazette of the US Patent and Trademark Office Patents* (1999).
- Hayashi, C. Y. & Lewis, R. V. Evidence from flagelliform silk cDNA for the structural basis of elasticity and modular nature of spider silks. *J. Mol. Biol.* **275**, 773–784 (1998).
- Gosline, J. M., Gurette, P. A., Ortlepp, C. S. & Savage, K. N. The Mechanical Design of Spider Silks: from Fibroin Sequence to Mechanical Function. *J. Exp. Biol.* **202**, 3295–3303 (1999).
- Vollrath, F. & Knight, D. P. Liquid crystalline spinning of spider silk. *Nature* **410**, 541–548 (2001).
- Bustamante, C., Smith, S. B., Liphardt, J. & Smith, D. Single-molecule studies of DNA mechanics. *Curr. Opin. Struct. Biol.* **10**, 279–285 (2000).

42. Waite, J. H., Vaccaro, E., Sun, C. & Lucas, J. M. Elastomeric gradients: A hedge against stress concentration in marine holdfasts? *Phil. Trans. R. Soc. Lond. B* **357**, 143–153 (2002).
43. Vollrath, F. *et al.* Compounds in the droplets of the orb spider's viscid spiral. *Nature* **345**, 526–528 (1990).
44. Vollrath, F. & Tillinghast, E. K. Glycoprotein glue beneath a spider web's aqueous coat. *Naturwissenschaften* **78**, 557–559 (1991).
45. Makarov, D. E., Wang, Z., Thompson, J. B. & Hansma, H. G. On the interpretation of force extension curves of single protein molecules. *J. Chem. Phys.* **116**, 7760–7765 (2002).
46. Shear, W. A., Palmer, J. M., Coddington, J. A. & Bonamo, P. M. A devonian spinneret: early evidence of spiders and silk use. *Science* **246**, 479–481 (1989).
47. Gatesy, J., Hayashi, C., Motriuk, D., Woods, J. & Lewis, R. Extreme diversity, conservation, and convergence of spider silk fibroin sequences. *Science* **291**, 2603–2605 (2001).
48. Kindt, J. H. *et al.* in *Atomic Force Microscopy in Cell Biology* (eds Jena, B. P. & Hoerber, H.) 213–230 (Academic, San Diego, 2002).
49. Hayashi, C. Y., Shipley, N. H. & Lewis, R. V. Hypotheses that correlate the sequence, structure, and mechanical properties of spider silk proteins. *Int. J. Biol. Macromol.* **24**, 271–275 (1999).
50. Guerette, P. A., Ginzinger, D. G., Weber, B. H. F. & Gosline, J. M. Silk properties determined by gland-specific expression of a spider fibroin gene family. *Science* **272**, 112–115 (1996).

#### Acknowledgements

We thank D. Bensimon for helping us discover that the force–distance curves are exponential, and H. Gaub, J. Fernandez, S. Fossey, M. Viani, R. Proksch, H. Li, and B. Smith for discussions. This work was supported by NSF MCB grants to H.G.H., NSF DMR grants to P.K.H. and to UCSB's Materials Research Laboratory; ARO DAAG55-98-1-0262 (C.Y.H.), the Robert A. Welch Foundation (D.E.M.), and Asylum Research, Santa Barbara.

Correspondence and requests for materials should be addressed to H.G.H.

#### Competing financial interests

The authors declare that they have no competing financial interests.